Structural Chemistry (2022) 33:1755–1769
https://doi.org/10.1007/s11224-022-02022-x

ORIGINAL RESEARCH

Molecular dynamic simulation suggests stronger interaction of Omicron-spike with ACE2 than wild but weaker than Delta SARS-CoV-2 can be blocked by engineered S1-RBD fraction

Dipannita Santra[1] · **Smarajit Maiti**[1,2]

Received: 16 March 2022 / Accepted: 26 July 2022 / Published online: 4 August 2022

Abstract

The SARS-CoV-2 claimed millions of lives, globally. Occurring from Wuhan (wild type) in December, 2019, it constantly mutated to Omicron (B.1.1.529), the predecessor to Delta. Omicron having ~ 32 spike mutations has variable infectivity-multiplicity-immuno-invasive properties. Understanding of its mutational effect on ACE2-binding/disease severity and developing preventive/therapeutic strategies are important. The binding affinities of Wuhan/Delta/Omicron spikes (PDB/GISAID/SWISS-MODEL) were docked (HADDOCK2.4) with ACE2 and compared by competitive-docking (PRODIGY). The protein structural stability was verified by kinetic-data/Ramachandran-plot (Zlab/UMassMedBioinfo). After several trials, a 59 amino acid (453ARG-510VAL) peptide-cut (Expasy-server) of the wild-type spike RBD with some desired mutants (THR500SER/THR500GLY/THR500ALA/THR500CYS) was blindly/competitively docked (PyMOL-V2.2.2) to block the Omicron-ACE2 binding. We examined molecular dynamic simulation (iMOD-server, with 9000 cycles/300 k-heating/1 atm pressure for system equilibration for 50 ns-run) of ACE2 and two CUTs with different SARS-CoV-2 variants. The binding-affinity of Omicron-ACE2 is slightly higher than the rest two in competitive docking setup. During individual (1:1) docking, Omicron showed little higher than wild type but much weaker binding affinity than Delta. Competitive docking suggests ten H-bonding (1.3–2.4 Å) with highly favorable energy values/Van-der-Walls-force/Haddock score for more stable-binding of Omicron-RBD with ACE2. Blind docking of different CUTs (wild/mutants) and Omicron to ACE2 completely rejected the Omicron-RBD from ACE2-target. The best blocking/binding affinity of −16.4 and −13 kcal/mole were observed in the case of THR500SER and THR500GLY, respectively, with multiple H-bonding 1.9–2.2 Å. These are supported by the MD-simulation results. So, the spike binding affinities were Delta > Omicron > wild in 1:1 docking with ACE2. Considering the wild type is non-existing nowadays, Omicron showed less ACE2 binding properties. The 59 cut of spike-RBD and its mutant THR500SER/THR500GLY may be further screened as universal blockers of this virus.

Keywords SARS CoV-2 · Wild type · Delta and Omicron variant · Comparative affinity · Preventive blocking/docking · 59 amino acid RBD cut

Introduction

The SARS-CoV-2 pandemic has been surging all over the world for 2 years. According to the statistical report of the World Health Organization (WHO), more than 260 million confirmed cases and over five million deaths have been reported [1]. The original (Wuhan) severe acute respiratory syndrome coronavirus 2 (SARS-CoV-2) was first identified at the end of December 2019 and was followed by a wave that peaked in July 2020 and ended in September 2020. SARS-CoV-2 evolved quickly and a variety of variants emerged.

✉ Smarajit Maiti
maitism@rediffmail.com

Dipannita Santra
dipannita.santra5@gmail.com

[1] Department of Biochemistry and Biotechnology, Cell and Molecular Therapeutics Laboratory, Oriental Institute of Science and Technology, Midnapore, India

[2] Agricure Biotech Research Society, Epidemiology and Human Health Division, Midnapore 721101, India

The WHO classifies them into three types: (a) variants of concern (VOCs), (b) variants of interest (VOIs), and (c) variants under monitoring (VUMs). The second wave, which was caused by the Beta (B.1.351/501Y.V2/20H) variant, peaked in January 2021 and ended in February 2021. The third wave, which peaked in July and ended in September 2021, was driven by Delta (B.1.617.2/478 K.V1/21A) variant [2]. In late November 2021, a new variant named Omicron (B.1.1.529/21 K) was designated as the fifth VOCs by the WHO. The emergence of the Omicron variant was first detected in South Africa, raising concerns based on at least 32 mutations in spike proteins. Many of which are located in the receptor binding domain (RBD). In addition, Omicron has 3 deletions and 1 insertion in the spike protein [3].

The effects of most of the remaining Omicron mutations are not known, resulting in a high level of uncertainty about how the full combination of deletions and mutations will affect viral behavior and susceptibility to natural and vaccine-mediated immunity. Several reports provide preliminary indications on more transmissibility, immune escape, and severity of the Omicron variant. But a recent report suggests, unlike previous variants, its less severe nature due to failure to penetrate the lung tissues in healthy individuals. But the nature of the severity in the co-morbid individuals is yet to be confirmed. It is also to be established the actual impact of Omicron in non-infected and non-vaccinated individuals. More data are needed to characterize the null or various factorial effects alone or in combination. Omicron has some deletions and more than 30 mutations, which overlap with those in the alpha, beta, gamma, or Delta VOCs [4]. N501Y increases binding to the ACE2 receptor to induce higher transmissibility [5] and the combination of N501Y and Q498R may increase binding affinity even more; however, other substitutions in the Omicron spike protein are expected to decrease binding to ACE2. Omicron does not infect cells deep in the lung tissues as readily as it does those in the upper airways, and after a few days, the concentration of virus in the lungs of animals infected with Omicron was at least ten times lower than that in rodents infected with other variants [6].Other studies reveals that Omicron may be over 10 times more contagious than the original virus or about 2.8 times as infectious as the Delta variant [7].

The Omicron variant, when combined with the H69/V70 deletion, the transmissibility, might be further increased [8]. H655Y is proximal to the furin cleavage site and may increase spike cleavage, which could also increase transmission. P681H has been shown to enhance spike cleavage, which could help transmission. This mutation is found in Alpha and an alternate mutation at this position (P681R) is found in Delta. Previous studies have clarified that D614G is associated with higher upper respiratory tract viral loads and younger age of patients [9–11].

So far, several drugs have been tested in COVID-19 for its mild, moderate, and severe conditions. And for preventive strategies, a significant number and types of vaccines have been used globally. Several reports reveal the sharp failure of the vaccines and that is demonstrated by the epidemiological or vaccinated patient's sera neutralization data. The investigator examined its sensitivity to 9 monoclonal antibodies (mAbs) clinically approved or in development, and to antibodies present in 115 sera from COVID-19 vaccine recipients or convalescent individuals [12]. Omicron was totally or partially resistant to neutralization by all mAbs tested. Sera from Pfizer or AstraZeneca vaccine recipients, sampled 5 months after complete vaccination, barely inhibited Omicron [12]. Booster Pfizer dose as well as vaccination of previously infected individuals generated an anti-Omicron neutralizing response, with titers 6- to 23-fold lower against Omicron than against Delta. We noted that the activity of 17 of the 19 antibodies tested were either abolished or impaired, including ones currently authorized or approved for use in patients [13]. In addition, we also identified four new spike mutations (S371L, N440K, G446S, and Q493R) that confer greater antibody resistance to B.1.1.529 [13]. Omicron subsequently and swiftly replaced the circulating Delta and other variants. The genome surveillance data shows the comparison between predicted and observed fractions of Omicron, Delta, and other variants. Omicron was estimated to be 4.2 times (95% confidence interval (CI) 2.1, 9.1) greater than that of the Delta variant. It was found 3.3 times more transmissible than the Delta variant. [14].

But it is evident that the hospitalization or the case fatality (CFR) is much lower in the Omicron infected cases. In earlier and also in recent periods, several angiotensin receptor blockers (ARBs) exhibited some protecting effects. In addition to the antihypertensive effects, these drugs manifested some anti-inflammatory effects also. The ARBs are found to be protective in severe acute respiratory syndrome caused by the virus. Moreover, in some cases, ACE-inhibitors and ARBs were also found to be associated with decreased mortality [15].

In this background, the blocking of the viral spike and the ACE2 binding was studied in the present study. A comparative in silico study was done to evaluate the ACE2 binding with Wuhan (wild type), Delta, and the Omicron variants of SARS CoV-2. Small peptides from the globally conserved spike variants were designed with or without mutations and docking effects were tested with ACE2 in the presence of the Omicron spike.

Materials and methods

Protein structure retrieval, prediction by analysis

The X-ray crystallography and electron microscopy structure were retrieved from RCSB Protein Data Bank (https://

www.rcsb.org) in PDB format. The PDB IDs used in this study were 4APH, 7CWN, and 7KRQ representing human angiotensin-converting enzyme 2 receptor (ACE2), human coronavirus (SARS CoV2) spike glycoprotein, and another variant of concern B.1.617.2 (now delta) spike protein, respectively. Recently, a new SARS-CoV-2 variant B.1.1.529 (Omicron) was detected in South Africa. The spike protein of the Omicron variant is characterized by at least 30 amino acid substitutions, three small deletions, and one small insertion. Notably, 15 of the 30 amino acid substitutions are in the receptor binding domain (RBD). There are also a number of changes and deletions in other genomic regions. H69-, V70-, G142-, V143, Y144-, and N211- of which 69/70 deletions resulted in the failure of the S-gene target. Other substitutions in the spike protein are A67V, T95I, Y145D, G339D, S371L, S373P, S375F, K417N, N440K, G446S, S477N, T478K, E484A, Q493R, G496S, Q498R, N501Y, Y505H, T547K, D614G, H655Y, N679K, P681H, N764K, D796Y, N856K, Q954H, N969K, and L981F. Of these, mutations at H655Y, N679K, and P681H in the S1-S2 furin cleavage site of the Omicron variant might be associated with increased transmissibility [16]. We manually prepared Omicron spike protein from wild-type SARS-COV-2 spike protein (PDB-7CWN). From our previous study, we prepared some short CUT segments with 84 amino acid sequences for analyzing the blocking between different nCoV2 and ACE2 receptor binding at RBD domain [17]. Here, we prepared a new short CUT segment from the previous 84 CUTs with 59 amino acids in two steps; CUT segment was prepared from the tertiary structure of 7CWN and the respective CUTs were subjected to SWISS-MODEL for tertiary structure prediction.

Structural modification

The selected PDB structures were found with different molecules like H2O and NAG, whereas COVID-19 spike glycoprotein showed with multiple NAG units at different positions. So, for molecular docking study studies, different attached molecules were removed from the receptor molecules and manually prepared spike proteins with exact amino acid position mutations using Pymol molecular visualization software [18]. After removal, receptor molecules are saved as a.pdb file for further analysis. After tertiary structure, prediction was performed to understand if mutation could elevate the binding affinity of the cut or not. One-point mutation was performed at THR500 position replacement with THR500SER named as CUT1 or T500S; THR500CYS as CUT2 or T500C; THR500GLY as CUT3 or T500G; and THR500ALA as CUT4 or T500A. For molecular docking study, different attached molecules were removed from the receptor molecules; manually prepared spike proteins with exact amino acid position mutations and different CUT segments were prepared using Pymol molecular visualization software [18]. After removal, receptor molecules were saved as a.pdb file for further analysis.

Ramachandran plot analysis

Ramachandran Plot server [19] was used for protein 3D quality structure assessment (https://zlab.umassmed.edu/bu/rama/). We observed the Ramachandran plot on the number of residues present in highly preferred regions and allowed regions; wild-type SARS-Cov2 94.5%, Delta 94.5%, and Omicron 94.402% were found as a very good quality structure. We also observe the Ramachandran plot of docked complexes and select the best structures (Table S4).

Molecular docking studies

Surface topology calculation of proteins

Protein pocket and cavity properties are characterized by the solvent accessibility factor. The second water molecule is restricted to entering after the first one occupies these areas. The CASTp (Computed Atlas of Surface Topography of Protein) (http://sts.bioe.uic.edu/castp/index.html?j_5e8c7bec25090) was used in the current study to characterize the pocket and cavity.

The molecular docking between human ACE2 and different mutated spike proteins was individually and competitive blind docking through HADDOCK 2.4 web server [20] to check the highest and lowest binding affinity with ACE2 receptor. Also, blind docking was performed of selected mutated CUTs with ACE2 and Omicron variants were performed on HADDOCK 2.4 server. We only analyze the binding of CUT segments with ACE2 and Omicron because our previous study already checked the binding affinity of CUT segments with SARS-CoV2. HADDOCK is an integrative platform for the modeling of biomolecular complexes. It supports a large variety of input data and deals with a large class of modeling problems including protein–protein, protein-nucleic acids, and protein–ligand complexes, including multi-body assemblies. It also allows to define specific unambiguous distance restraints (e.g., from MS cross-links) and supports a variety of other experimental data including NMR residual dipolar couplings, pseudo contact shifts, and cryo-EM maps. It calculates the docking transformation between two molecules to get the best molecular interface complementary, which finds out the binding affinity between biomolecule complexes. HADDOCK analyzes the protein–protein docking from different angles through HADDOCK score, RMSD from the overall lowest-energy structure, Van der Waals energy, electrostatic energy, desolvation energy, restraints violation energy, buried surface area, and *Z*-score.

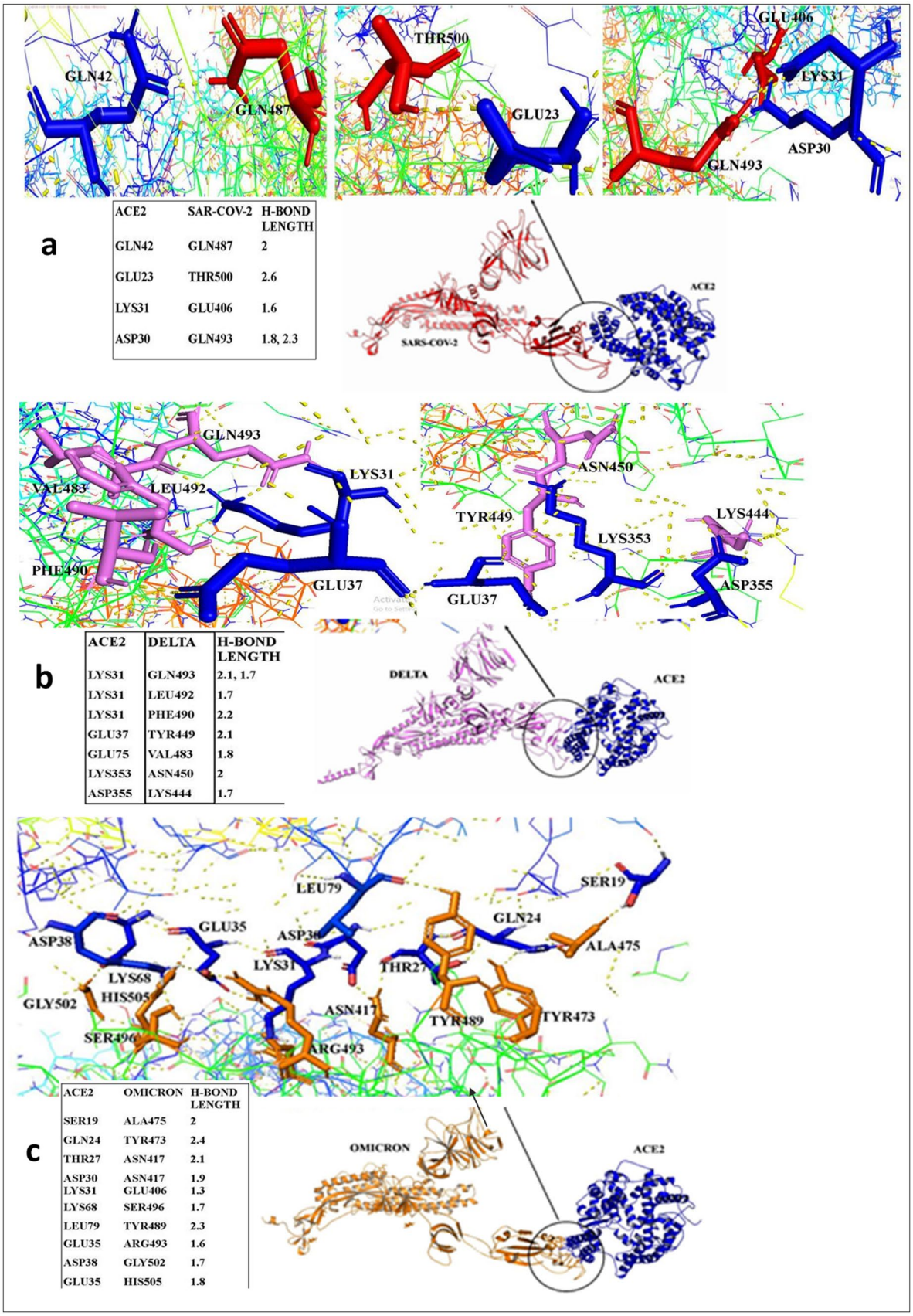

ACE2	SAR-COV-2	H-BOND LENGTH
GLN42	GLN487	2
GLU23	THR500	2.6
LYS31	GLU406	1.6
ASP30	GLN493	1.8, 2.3

ACE2	DELTA	H-BOND LENGTH
LYS31	GLN493	2.1, 1.7
LYS31	LEU492	1.7
LYS31	PHE490	2.2
GLU37	TYR449	2.1
GLU75	VAL483	1.8
LYS353	ASN450	2
ASP355	LYS444	1.7

ACE2	OMICRON	H-BOND LENGTH
SER19	ALA475	2
GLN24	TYR473	2.4
THR27	ASN417	2.1
ASP30	ASN417	1.9
LYS31	GLU406	1.3
LYS68	SER496	1.7
LEU79	TYR489	2.3
GLU35	ARG493	1.6
ASP38	GLY502	1.7
GLU35	HIS505	1.8

◂**Fig. 1** Individual molecular docking of ACE2 receptor and spike glycoproteins. **a** ACE2 with wild-type SARS-COV-2 binding; **b** ACE2 with Delta variant; **c** ACE2 with Omicron variant. The binding between ACE2 and three spike proteins shown in various position of amino acids

Docking result and binding affinity analysis of different docked molecules

Each sets of molecular docking were analyzed using PyMol molecular visualization software [18]. The presentation of docking structures and interactive bonds were represented through technical and transparent surface analysis mainly. To understand the binding between different docked molecules, each pairs was individually subjected to PRODIGY tool on HADDOCK server. PRODIGY was used to analyze the binding affinity of protein–protein and protein-small molecule complexes and also allows classifying crystallographic interfaces as biological or not [21]. The best structures for the docking result were accepted. Based on the previous study for complete displacement of nCOV2 spike protein from ACE2 RBD through the CUT segment, the highest binding affinity of CUTs with ACE2 RBD and Omicron variant, the best CUT was selected for further analysis. Binding affinity quantifies the binding strength of ligand to a protein.

Evaluation of H-bonding in a competitive docking analysis

Observation of the H-bonding length of amino acid residues between the ACE2 receptor and the original SARS-CoV-2 isolate Wuhan-Hu-1, the Delta mutant, and Omicron mutant demonstrated by PyMol-visualized system to recognize the H-bond length between amino acid residues short or long. The H-bond interaction in short CUT segments with ACE2 and Omicron spike protein was also observed.

Energetic and kinetic data analysis

During the generation of the HADDOCK score, cluster-size-based RMSD values and other bond energy values, i.e., Van der

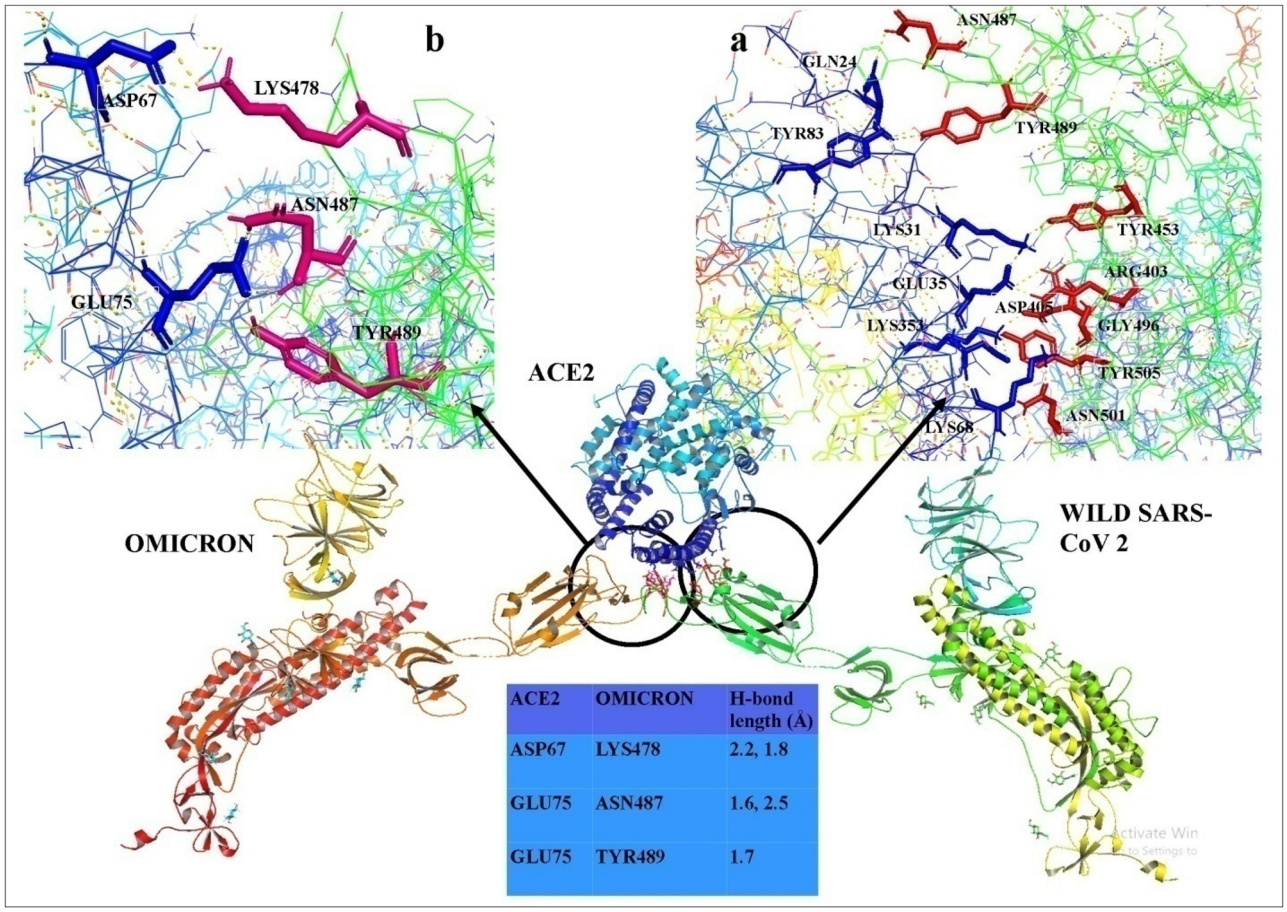

Fig. 2 The superposition of the docked complexes of SARS-COV2 wild-type and Omicron spike proteins binding with human ACE2 receptor is presented. (**a**) The enlarged panel on the right side shows the interacting amino acid residues in colored sticks in which wild-type SARS-CoV-2 is red; (**b**) the left side shows the Omicron mutant variant in pink. In both enlarged colored sticks, ACE2 receptor indicated with blue. Omicron variant interacts with ACE2 receptor in 3 different amino acid positions which was indicated in table form

Waals, electrostatic, and desolvation energy, were evaluated. Binding affinity (ΔG (kcal mol^{-1}) dissociation constant [Kd (M) at 25 °C]) explains the strength and the affinity of the interactions.

Molecular dynamic simulation study of different VOCs of SARS-CoV 2 with human ACE2 and two CUT sequences

Based on the docking results, we performed molecular dynamic analysis studies on the selected lowest energy valued and best-posed docking complex. The MD simulations were carried out by iMod server (iMODS) (http://imods.chaconlab.org/) [22] at 300 K constant temperature, 1 atm constant pressure at molecular mechanics level. The iMod server gives a convenient interface for this enhanced normal mode analysis (NMA) methodology in inner coordinates. The web interface is very spontaneous and responsive to all major browsers and even to modern mobile appliances. Users can perform NMA or molecular dynamics to simulate feasible trajectories between two conformations and interactively explore in 3D the resulting structures, trajectories, animations, and even for large macromolecules. Finally, 50 ns molecular dynamic simulation was carried out for all the complexes, such as different VOCs of SARS-CoV 2 with ACE2 and two CUT 59 sequences (wild 59 and T500S) with Omicron variants.

For structural stability analysis for docking and simulations, providing an RMSD (root mean square deviation) or root-mean-square deviation is a standard measure of structural distance between two proteins. To simulate feasible transitions, the initial structure is iteratively deformed along the lowest modes while the root mean square deviation (RMSD) for a target structure is minimized. Two initial superimposition methods can be selected: either global [23] or local [24]. Whereas the former considers all atoms for the RMSD, the latter favors the overlap between most similar regions.

Results and discussion

In the current study, we are presenting by the in silico study the comparative analysis of binding/docking parameters of wild-type SARS CoV-2, Delta, and Omicron variants with human ACE2. We further analyzed the effects of the 59 amino acids of the RBD fraction of SARS CoV-2 and its various mutants, THR500SER/GLY/ALA/CYS docking/blocking effects on ACE2 Omicron spike binding. Besides the individual spike variant binding with ACE2, comparative/combined binding of different spikes was also evaluated to predict which is more infective/transmissible. Our present results suggest a few considerations.

Table 1 H-bonding patterns and bond length during different competitive binding of SARS-CoV-2 variants: wild (Wuhan), Delta, and Omicron spikes with human ACE2

Competitive HADDOCK	*ACE2*	*Wild SARS-COV-2*	*H-bond length (Å)*
1. ACE2 + WILD SARS-COV-2 + Omicron	TYR83	TYR489	2.4
	GLN24	AS487	2.5
	LYS31	TYR453	2.3
	GLU35	ARG403	2.7, 1.5
	LYS353	ASP405	2.1
	ASP38	TYR505	2.7
	LYS68	GLY496	1.7
	LYS68	ASN501	1.7
	ACE2	*Omicron*	*H-bond length (Å)*
	ASP67	LYS478	2.2, 1.8
	GLU75	ASN487	1.6, 2.5
	GLU75	TYR489	1.7
2.ACE2 + DELTA + Omicron	*ACE2*	*Delta*	*H-bond length (Å)*
	GLN42	ASP571	2.4
	ASP38	ARG567	2.5, 1.6, 1.9
	LYS353	GLN563	2.1
	ACE2	*Delta*	*H-bond length (Å)*
3.ACE2 + DELTA + Omicron + WILD SARS-COV-2	GLU329	LYS558	1.5
	TYR41	GLN563	2.5
	TYR83	LYS462	1.7
	SER19	GLU471	2.1
	ACE2	*Omicron*	*H-bond length (Å)*
	GLU87	ARG498	1.6, 2
	LYS112	ALA372	2.1

SARS-COV2 and Omicron spike proteins binding with human ACE2 receptor

The spike glycoprotein of both variants initially binds to the angiotensin converting enzyme 2 (ACE2) present at the host cell surface and then the viral entry gradually proceeds. This ACE2 attachment site remains folded until it reaches the receptor. Just before ACE2 attachment in SARS-CoV2 spike, the protein's flexible part becomes unfolded and the attachment site becomes exposed [25]. Individual docking of ACE2 and three different spike protein results were observed (Fig. 1). According to the competitive multi-docking studies between ACE2-SARSCoV2–Omicron showed the highest docking score of -194.5 ± 5.1. The cumulative energy calculation of Van der Waals energy, desolvation energy, and electrostatic energy represented the negative value of -98.0 ± 9.9, -50.9 ± 13.4, and -315.3 ± 105.1, respectively (Table S1).

Electrostatic energy represents the potential energy of a system placed within the time-invariant electric field [26] where the positive value indicates the repulsion and the negative value indicates the surface attraction between two molecules [27]. Here, SARS-CoV-2 showed higher binding affinity with ACE2 with a value −9 ΔG (kcal mol^{-1}) and it also showed some dissociation constant value of 2.50E-07 (Kd(M) at 25 °C). In contrast, molecular docking with ACE2 and Omicron showed comparable binding affinity of −7.4 ΔG (kcal mol^{-1}) (Table S2) at the binding site. The active site of ACE2 comprises different amino acids, i.e., TYR83, GLN24, LYS31, GLU35, LYS353, ASP38, and LYS68, with which interaction of TYR489, AS487, TYR453, ARG403, ASP405, TYR505, GLY496, and ASN501 different amino acids of SARS-CoV2 binding sites were observed, respectively (Fig. 2; Table 1).

The active site of ACE2 comprises different amino acids, i.e., ASP67 and GLU75, with which interaction of LYS478,

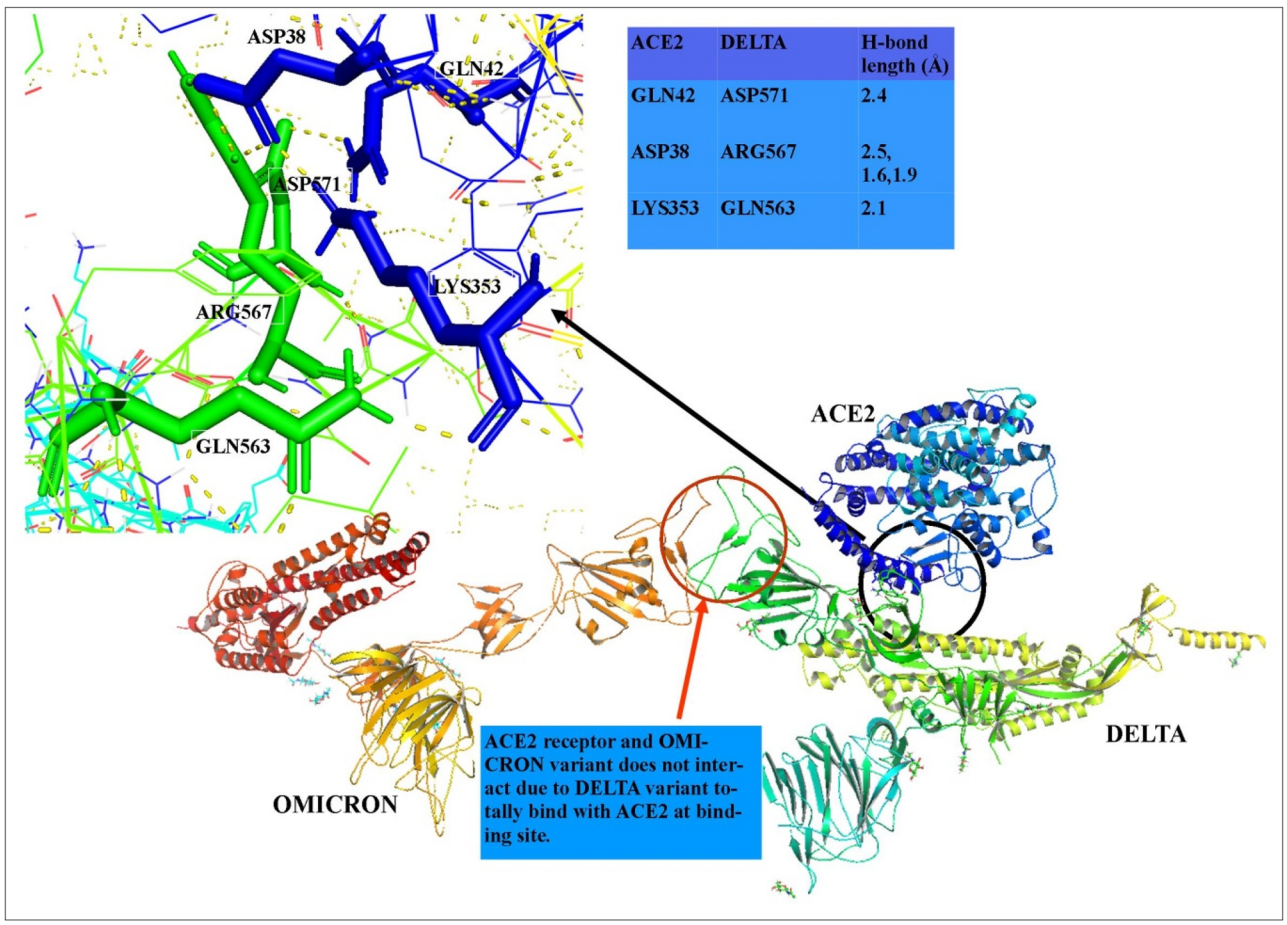

ACE2	DELTA	H-bond length (Å)
GLN42	ASP571	2.4
ASP38	ARG567	2.5, 1.6,1.9
LYS353	GLN563	2.1

Fig. 3 The superposition of the docked complexes of Delta and Omicron spike proteins binding with human ACE2 receptor was presented. The enlarged panel on the left side shows the interacting amino acid residues in colored sticks in which Delta is in green color and ACE2 receptor indicated with blue. On the other hand, Omicron variant does not interact with ACE2 receptor. Delta variant interact with ACE2 receptor in 3 different amino acid positions which was indicated in table form

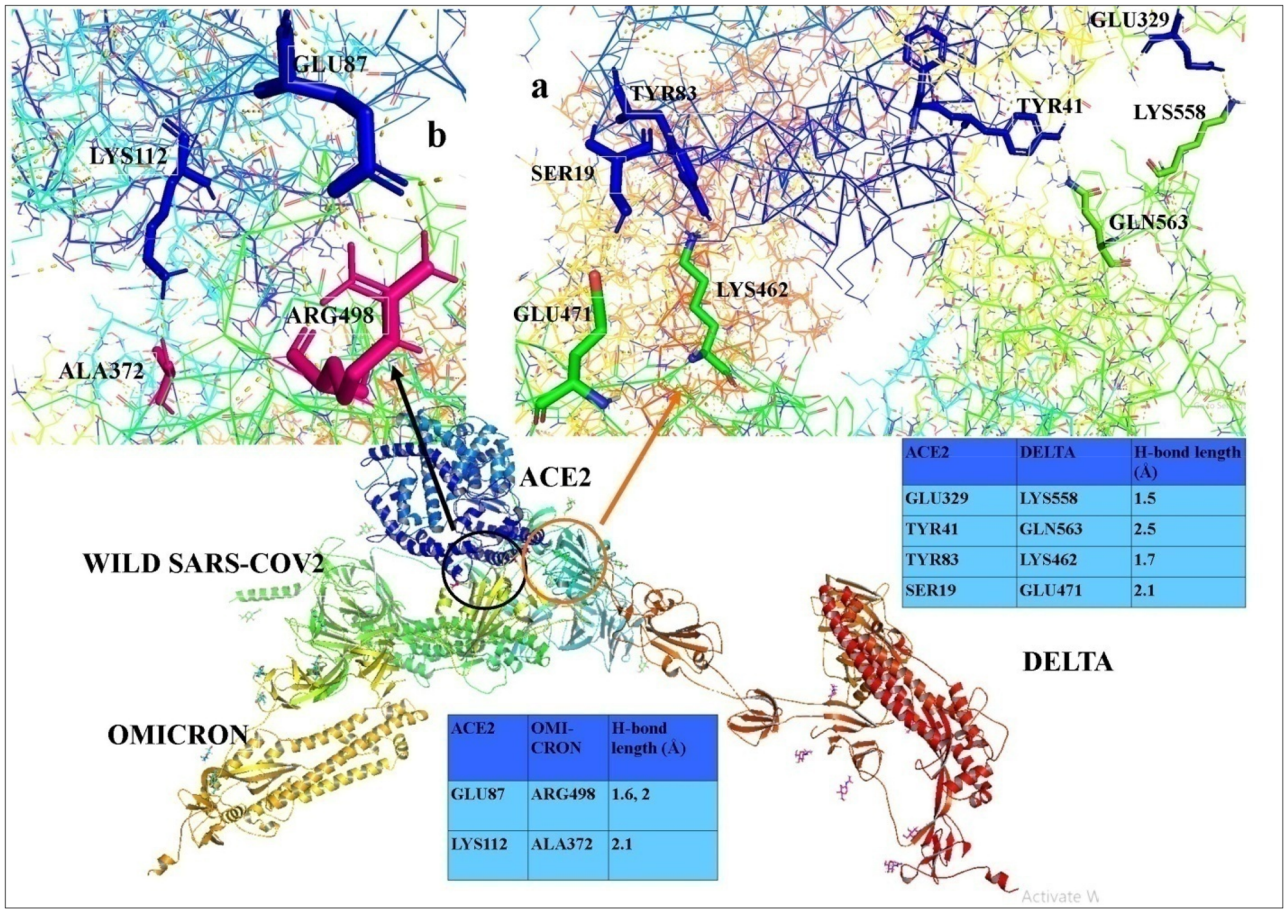

Fig. 4 The superposition of the docked complexes of wild-type SARS-CoV-2, Delta, and Omicron spike proteins binding with human ACE2 receptor was presented. (**a**) The enlarged panel on the right side shows the interacting amino acid residues in colored sticks in which Delta is in green color and ACE2 receptor indicated with blue; (**b**) the left side shows the interacting amino acid residues in colored sticks in which Omicron variant is in pink and ACE2 receptor is in blue. Wild-type SARS-CoV-2 totally blocked by other two types of variant and do not interact with ACE2 at binding site. Delta variant interact with ACE2 receptor in 4 different amino acid positions and Omicron variant interact with ACE2 receptor in 2 different amino acid positions which was indicated in table form. So, the binding comparison between 3 spike glycoproteins with ACE2 receptor and Delta variant has highest binding positions with receptor than other 2 types of spike glycoproteins

ASN487, and TYR489 different amino acids of Omicron variant binding sites were observed, respectively (Fig. 2; Table1). At the surface of ACE2 and spike glycoprotein interaction, all the amino acids interact with each other with the formation of H-bonds (Table 1).

Delta and Omicron spike proteins binding with human ACE2 receptor

Molecular docking with Delta variant and Omicron variant with the ACE2 receptor revealed the highest docking scores of -137.6 ± 12.1. The calculation of Van der Waals energy, desolvation energy, and electrostatic energy represented the negative value of -80.4 ± 4.0, -31.8 ± 2.9, and -284.8 ± 64.1, respectively (Table S1). Here, DELTA variant showed higher binding affinity with ACE2 with a value -9.7 ΔG (kcal mol^{-1}) and it also showed some dissociation constant value of 7.70E-08 (Kd(M) at 25 °C) (Table S2). Contrarily, Omicron variant did not show any binding affinity against ACE2 in the presence of DELTA. It could be possible that the 15 mutations of RBD Omicron are not evenly distributed in RBD, but rather crowed in its RBM with 10 residues, viz., N440K, G446S, S477N, T478K, E484A, Q493K, G496S, Q498R, N501Y, and Y505H [28]. For that reason, Omicron variant has lower binding affinity than DELTA.

The active site of ACE2 comprises different amino acids, i.e., GLN42, ASP38, and LYS353, with which interaction of ASP571, ARG567, and GLN563 different amino acids at the Delta binding sites were observed, respectively (Fig. 3;

Table 2 Data of HADDOCK competitive binding and blocking of human ACE2 binding by the wild SARS-CoV-2 spike RBD fraction of 59 amino acid and its different mutants, i.e., TYR500SER, TYR500ALA, TYR500GLY, and TYR500CYS

HADDOCK parameters	Cluster name	HADDOCK score	Cluster size	RMSD from the overall lowest-energy structure	Van der Waals energy	Electrostatic energy	Desolvation energy	Restraints violation energy	Buried surface area	*Z*-score
1. ACE2 + WILD 59 + OMICRON	Cluster 2	−175.1 ± 13.8	17	46.8 ± 4.0	−116.1 ± 18.8	−272.1 ± 60.5	−64.7 ± 7.0	601.6 ± 148.7	3631.3 ± 165.7	−0.8
	Cluster 3	−167.8 ± 7.1	11	32.9 ± 7.3	−125.2 ± 17.0	−375.9 ± 92.9	−40.0 ± 9.0	725.6 ± 193.6	3803.9 ± 250.7	−0.5
	Cluster 1	−166.2 ± 16.2	23	27.8 ± 10.7	−114.7 ± 10.6	−363.6 ± 66.9	−44.3 ± 10.2	655.3 ± 52.1	3666.6 ± 171.6	−0.5
	Cluster 4	−100.7 ± 17.4	4	53.3 ± 1.6	−82.2 ± 6.5	−298.1 ± 59.5	−51.6 ± 6.7	926.7 ± 71.5	2918.6 ± 117.4	1.7
2. ACE2 + MUTANT 59 + OMICRON	Cluster 1	−163.1 ± 13.8	15	23.5 ± 6.1	−121.9 ± 15.2	−247.0 ± 63.0	−49.8 ± 2.6	579.9 ± 99.6	3408.9 ± 185.0	−1
	Cluster 3	−155.8 ± 8.8	8	27.4 ± 13.2	−108.9 ± 10.8	−332.9 ± 53.8	−38.6 ± 8.8	582.4 ± 122.0	3462.3 ± 107.1	−0.5
	Cluster 2	−154.6 ± 21.0	9	19.3 ± 3.2	−105.4 ± 18.2	−226.9 ± 50.7	−55.2 ± 5.0	514.7 ± 120.1	3315.5 ± 259.2	−0.5
	Cluster 5	−145.3 ± 4.2	4	21.2 ± 7.7	−97.1 ± 15.5	−263.4 ± 88.1	−51.1 ± 6.0	556.0 ± 106.3	3120.4 ± 252.1	0.2
	Cluster 4	−119.6 ± 12.0	5	19.5 ± 6.4	−84.3 ± 2.8	−333.1 ± 93.8	−51.6 ± 7.1	829.3 ± 48.3	3084.3 ± 150.5	1.9
3. ACE2 + T500GLY + OMICRON	Cluster 6	−163.6 ± 9.4	5	26.4 ± 9.7	−100.6 ± 11.3	−293.0 ± 87.5	−50.0 ± 7.5	455.7 ± 28.7	3450.5 ± 189.1	−1.6
	Cluster 1	−154.4 ± 9.5	10	31.2 ± 3.2	−113.3 ± 14.0	−369.7 ± 131.2	−45.4 ± 15.5	781.8 ± 162.4	3409.0 ± 134.9	−0.6
	Cluster 3	−151.5 ± 2.1	7	44.2 ± 6.7	−115.9 ± 13.7	−214.2 ± 30.8	−56.1 ± 6.5	632.8 ± 115.7	3684.8 ± 273.1	−0.3
	Cluster 2	−145.4 ± 10.3	7	32.4 ± 5.3	−95.1 ± 7.8	−402.7 ± 63.6	−52.3 ± 8.4	824.6 ± 23.0	3449.7 ± 164.2	0.3
	Cluster 4	−142.3 ± 10.4	7	34.0 ± 6.1	−92.2 ± 9.3	−375.9 ± 101.4	−36.1 ± 8.0	612.1 ± 42.3	3542.4 ± 169.4	0.6
	Cluster 5	−133.4 ± 21.6	6	33.5 ± 5.0	−92.7 ± 5.3	−272.9 ± 32.7	−53.6 ± 5.0	675.1 ± 169.7	3221.3 ± 173.1	1.6
4. ACE2 + T500ALA + OMICRON	Cluster 1	−174.0 ± 11.9	13	46.1 ± 5.2	−106.4 ± 8.5	−314.5 ± 99.0	−58.8 ± 10.4	541.6 ± 27.0	3543.3 ± 178.1	−1.4
	Cluster 3	−161.5 ± 9.0	9	32.4 ± 4.2	−121.1 ± 11.7	−322.9 ± 73.0	−41.3 ± 6.2	655.1 ± 68.0	3491.0 ± 222.5	−0.8
	Cluster 4	−149.5 ± 8.8	7	37.0 ± 3.2	−110.0 ± 15.3	−275.9 ± 65.1	−47.6 ± 5.6	633.0 ± 94.5	3535.8 ± 404.0	−0.2
	Cluster 2	−147.3 ± 16.3	10	35.6 ± 8.8	−108.1 ± 14.2	−343.2 ± 60.4	−34.0 ± 6.3	635.6 ± 121.4	3588.2 ± 105.4	−0.1
	Cluster 5	−131.1 ± 13.9	6	38.1 ± 0.6	−82.8 ± 14.4	−441.0 ± 54.2	−42.3 ± 5.4	821.9 ± 121.8	3335.9 ± 42.5	0.7
	Cluster 6	−108.5 ± 32.7	4	39.5 ± 5.9	−91.2 ± 9.1	−298.1 ± 81.1	−40.5 ± 8.2	828.5 ± 152.9	2915.9 ± 195.8	1.7
5. ACE2 + T500CYS + OMICRON	Cluster 5	−172.2 ± 26.8	4	8.6 ± 6.4	−106.5 ± 13.7	−391.1 ± 95.5	−46.1 ± 10.8	585.7 ± 119.2	3817.6 ± 377.4	−1
	Cluster 1	−162.4 ± 15.5	10	27.6 ± 9.0	−108.3 ± 17.5	−303.4 ± 130.3	−54.3 ± 14.5	608.6 ± 74.4	3530.5 ± 284.7	−0.7
	Cluster 2	−159.7 ± 16.9	9	27.3 ± 3.4	−105.4 ± 4.9	−324.2 ± 52.7	−45.9 ± 6.8	564.0 ± 147.4	3345.2 ± 152.7	−0.6
	Cluster 3	−127.2 ± 19.2	5	28.0 ± 7.1	−96.8 ± 5.2	−315.1 ± 71.0	−36.7 ± 6.0	694.1 ± 113.2	3411.4 ± 349.6	0.5
	Cluster 4	−93.5 ± 32.7	4	23.2 ± 6.7	−92.1 ± 15.1	−249.0 ± 45.7	−34.6 ± 7.1	829.2 ± 110.1	2651.1 ± 368.2	1.7

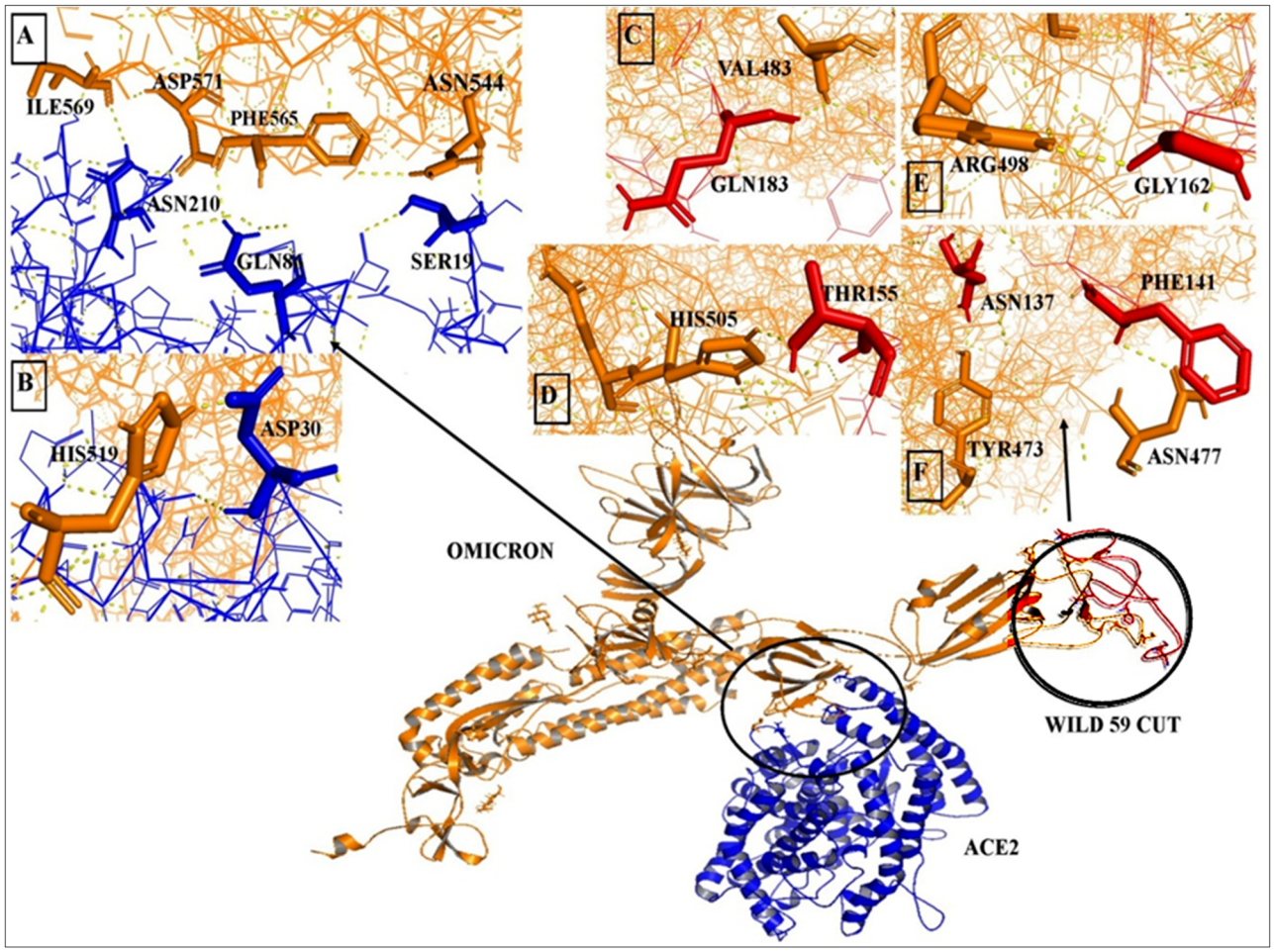

Fig. 5 The molecular docking of ACE2, Omicron variant, and mutant 59 cut. (**A** and **B**) The enlarged panel on the left side shows the interacting amino acid residues in colored sticks in which ACE2 is in blue and Omicron variant is in orange; (**C**, **D**, **E**) the enlarged panel on right side shows the interacting amino acid residues in which Omicron is in orange and mutant 59 cut is in green

Table 1). The H-bond length is also observed between amino acid residues (Table 1). On the other hand, molecular docking with ACE2 and Omicron showed no binding affinity and no binding occurs (Table S2).

Comparative study between 3 spike proteins binding with human ACE2 receptor

According to the docking results between ACE2, Delta, Omicron, and wild-type SARS-CoV-2, it showed the highest docking score value of -250.8 ± 19.4. The calculation of Van der Waals energy, desolvation energy, and electrostatic energy represented the negative values of -157.9 ± 11.4, -451.1 ± 46.0, and -63.6 ± 7.8, respectively (Table S1). The binding affinity of DELTA and Omicron with ACE2 was -7.1 and -9.9, respectively (Table S2). But molecular docking with ACE2 and wild-type SARS-CoV2 showed no binding affinity. From the above two results, we analyze that Delta has a stronger binding affinity with ACE2 than wild-type SARS-CoV-2 and Omicron. When we studied MD stimulation of ACE2 binding affinity with 3 different strains together, Omicron variant showed comparable binding affinity with human ACE2 in comparison with Delta strain.

According to Bloom et al. [29], it was found that 9 RBD Omicron mutations (S371L, S373P, S375F, K417N, G446S, E484A, G496S, Q498R, Y505H) should decrease the binding affinity to ACE2 while the other 6 mutations (G339D, N440K, S477N, T478K, Q493K, N501Y) should increase the binding affinity, resulting in a challenge of predicting its transmissibility and potential immune evasion risk. The binding site of ACE2 comprises different amino acids, i.e., GLU329, TYR41, TYR83, and SER19, with which interaction of LYS558, GLN563, LYS462, and GLU471 different amino acids of Delta binding sites were observed, respectively (Fig. 4; Table 1). The binding site of ACE2 comprises different amino acids, i.e., GLU87 and LYS112, with which interaction of ARG498 and ALA372 different amino acids at the Omicron binding sites were observed,

respectively (Fig. 4; Table 1). The H-bond length is also observed between amino acid residues (Table 1).

Measurement of binding affinity and kinetics of different CUT segment

Here, we investigate the blind docking of wild 59, T500S, T500C, T500G, and T500A interaction with ACE2 and Omicron showed the docking score value of $-175.1 \pm 13.8, -163.1 \pm 13.8, -172.2 \pm 26.8, -163.6 \pm 9.4$, and -174.0 ± 11.9, respectively (Table 2). According to binding affinity result, the binding affinity between wild 59 segments and Omicron variant was −12.5 ΔG (kcal mol^{-1}), T500S and Omicron variant −16.4 ΔG (kcal mol^{-1}), T500C and Omicron variant −12.2 ΔG (kcal mol^{-1}), T500G and Omicron variant −13 ΔG (kcal mol^{-1}), and T500A and Omicron variant −12.3 ΔG (kcal mol^{-1}) (Table S2).

Among the mutated CUT segment, we showed that the best binding affinity between CUTs and spike protein was −16.4 ΔG (kcal mol^{-1}) because the lower energy and higher negative value means the higher stability of the complex. Due to the sequence shorting, it may be that T500S cut have higher binding affinity than 84 cut segments. So, we choose only T500S cut segment for further analysis and wild 59 cut segment as a control. After analyzing the H-bond pattern, T500S cut showed 6 interactions with Omicron spike protein at RBD site ranging from 1.9 to 2.1 Å, whereas wild 59 cut showed 5 interactions ranging from 1.9 to 2.8 Å. The binding affinity values and H-bond interactions of T500S were comparatively higher than the wild 59 cut.

The interaction site of T500S cut comprises different amino acids ASN137, TYR 185, VAL 187, ASN 164, and SER 154 with which interaction of ASN450, TYR501, PRO499, CYS488, GLY485, and ALA484 different amino acids of Omicron binding sites were observed, respectively (Fig. 5). Our previous study analyzed the CUT segments of 84 amino acids after molecular docking with ACE2 receptor and SARS-CoV-2; the docked structures were either partial or complete interactive distortions of spike glycoprotein from ACE2 receptor were observed. But when we observed the docking structure of T500S cut segment, Omicron, and ACE2, T500S cut binds at RBD site of Omicron and ACE2 binds at a different position of Omicron not in the RBD active site. The docking structure of WILD59 segment Omicron and ACE2 was shown WILD59 segment binds at RBD site instead of the ACE2 receptor (Fig. 6).

Molecular dynamics simulation

The result of molecular dynamics simulation and normal mode analysis (NMA) of different docked complexes of ACE2 and different variants of SARS-CoV 2 is illustrated in Fig. 7. The simulation study was conducted to determine the movements of protein molecules. The main-chain deformability graph of the three complexes is shown in S-Figure:

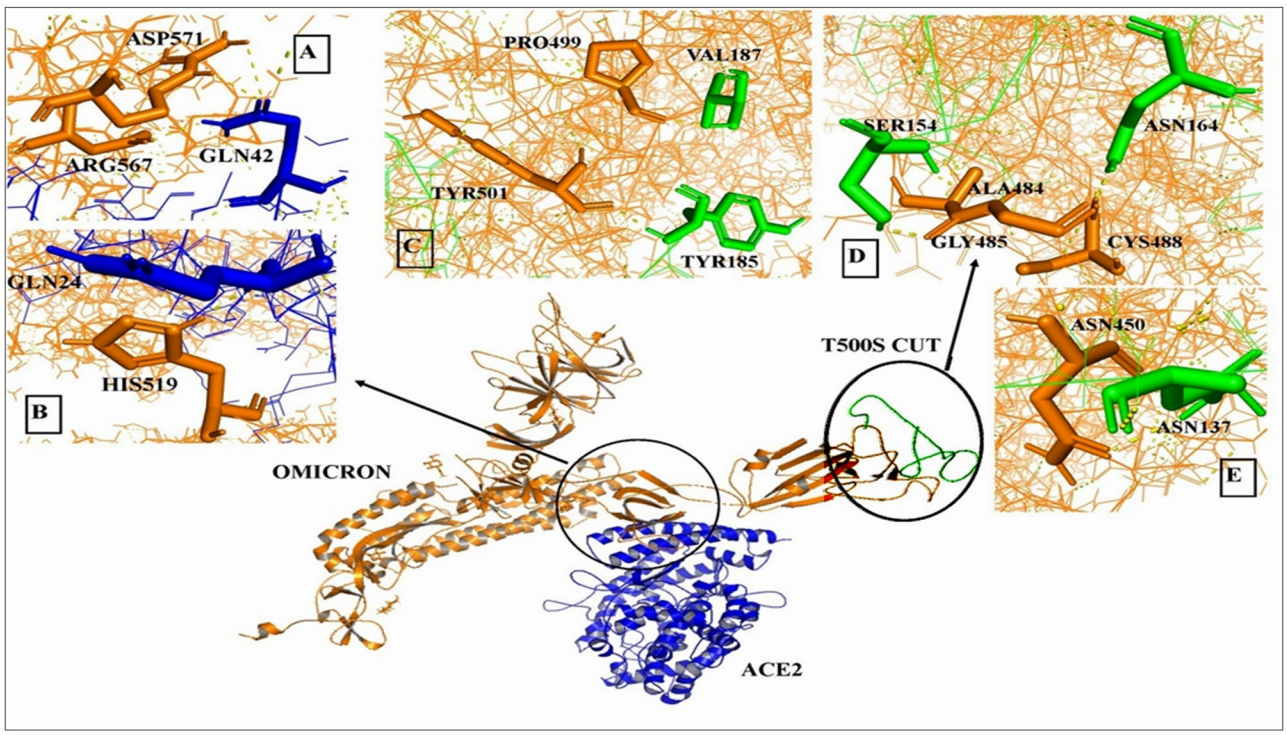

Fig. 6 The molecular docking of ACE2, Omicron variant, and wild 59 cut was presented. (**A** and **B**) The enlarged panel on the left side shows the interacting amino acid residues in colored sticks in which ACE2 is in blue and Omicron variant is in orange; (**C**, **D**, **E**, **F**) the enlarged panel on right side shows the interacting amino acid residues in which Omicron is in orange and Wild 59 cut is in red

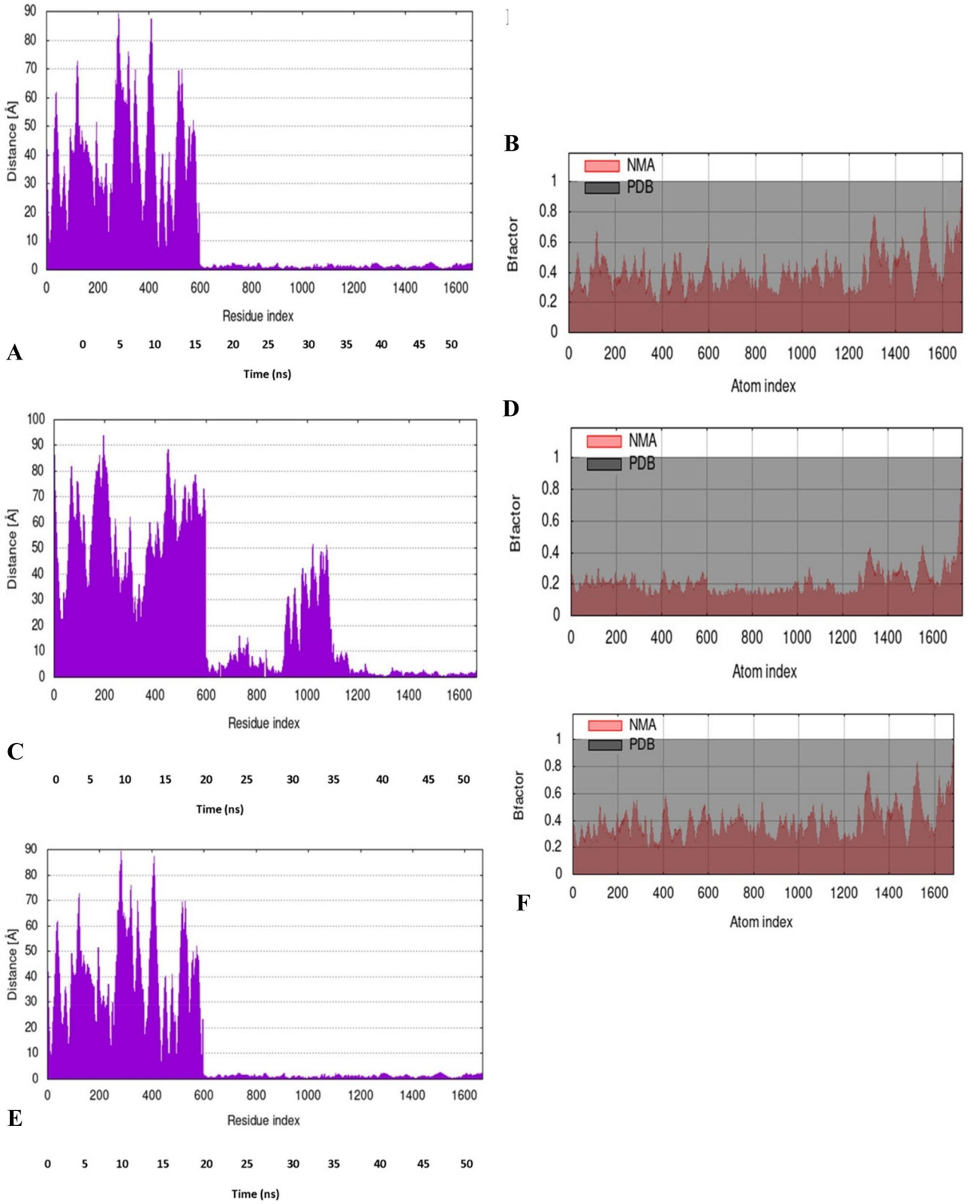

Fig. 7 The results of molecular dynamics simulation of different variant of SARS-CoV 2 and ACE2 docked complex. **A**, **B** RMSD plot and B-factor graph of wild-type SARS-CoV2 and ACE2; **C**, **D** RMSD plot and B-factor graph of Delta and ACE; **E**, **F** RMSD plot and B-factor graph of Omicron and ACE2

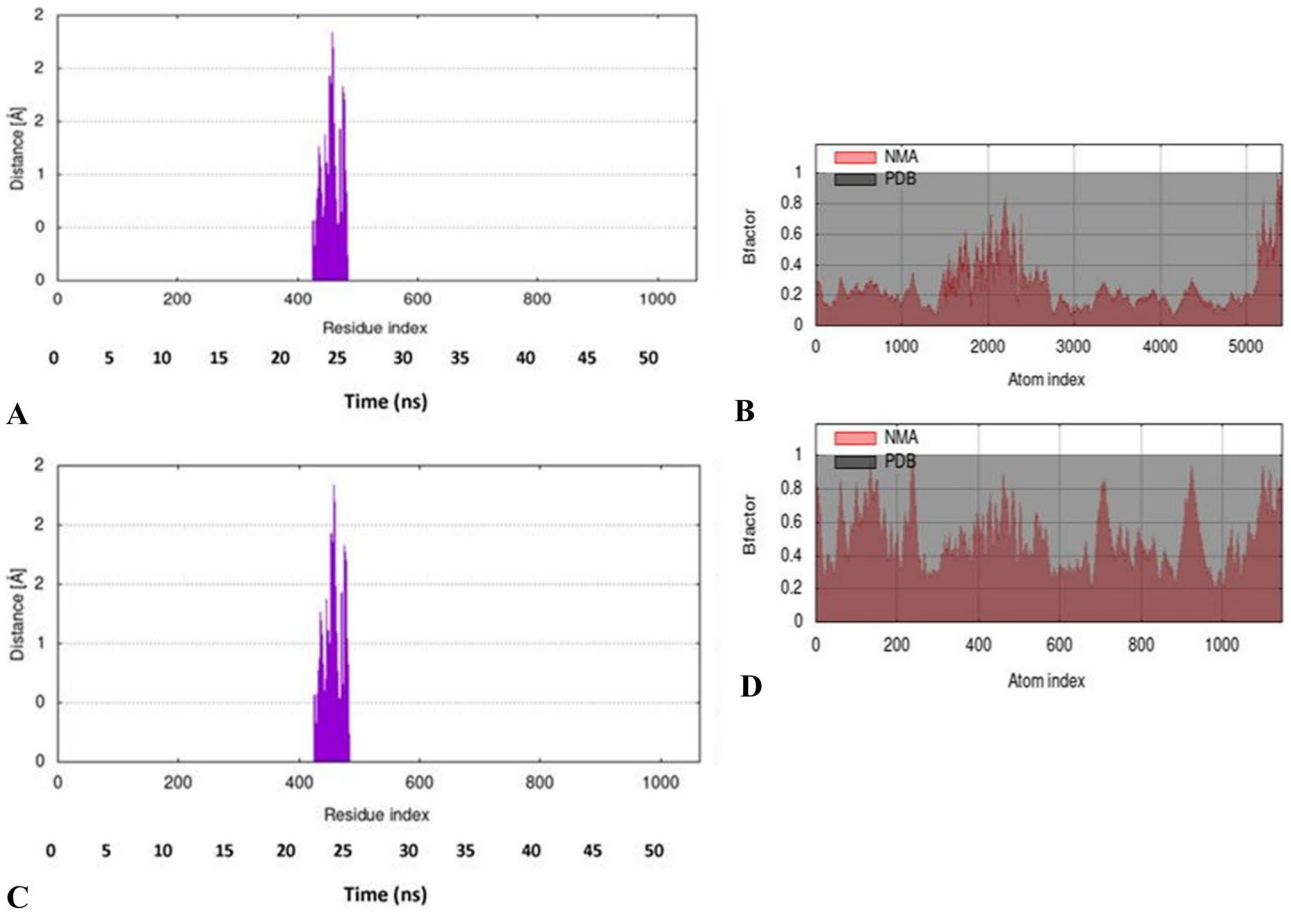

Fig. 8 The results of molecular dynamic simulation of two CUT 59 sequence with Omicron variant docked complex. **A**, **B** RMSD plot and B-factor graph of wild 59 CUTs and Omicron; **C**, **D** RMSD plot and B-factor graph of T500S 59 CUT sequence and Omicron

(1) illustrating the peaks which represent the regions of the protein with deformability. The locations with hinge regions have high deformability. The B-factor is a measure for flexibility in a protein and quantifies the uncertainty of each. The B-factor values calculated by normal mode analysis are proportional to the root mean square shown in Fig. 7. B-factor values quantify the uncertainty of each atom. The B-factor graph gives a clear visualization of the relation of the docked complex between the NMA and the PDB sector. The covariance matrix between the pairs of residues is shown in S-Figure: (1) indicating their correlations (correlated motion indicated by red color; uncorrelated motion indicated by white color; anti-correlated motion indicated by blue color).

We also examined the molecular dynamic simulation of wild 59 CUTs and T500S 59 CUTs with Omicron variant is illustrated in Fig. 8. The B-factor is a measure for flexibility in a protein and quantifies the uncertainty of each. The B-factor values calculated by normal mode analysis are proportional to the root mean square shown in Fig. 8. B-factor values quantify the uncertainty of each atom. The B-factor graph gives a clear visualization of the relation of the docked complex between the NMA and the PDB sector. The main-chain deformability graph of the three complexes is shown in S-Figure: (2) illustrating the peaks which represent the regions of the protein with deformability. The locations with hinge regions have high deformability. The covariance matrix between the pairs of residues is shown in S-Figure: (2) indicating their correlations (correlated motion indicated by red color; uncorrelated motion indicated by white color; anti-correlated motion indicated by blue color). So, all our docking complexes are in stable form.

The Omicron RBD shows weaker binding affinity than the currently dominant Delta variant to human ACE2 [28]. Here, we experimentally measured how all amino acid mutations to the RBD affect expression of folded protein and its affinity for ACE2. Most mutations are deleterious for RBD expression and ACE2 binding. But a substantial number of mutations are well tolerated or even enhance ACE2 binding, including ACE2 interface residues that vary across

SARS-related coronaviruses. However, we find no evidence that these ACE2-affinity-enhancing mutations have been selected in current SARS-CoV-2 pandemic isolates [30].

The report reveals that infection with Omicron caused an enhancement of Delta virus neutralization, which increased 4.4-fold. This may result in decreased ability of Delta to re-infect those individuals [31]. Omicron mutations enhance infectivity and reduce antibody neutralization of SARS-CoV-2 virus-like particles [32]. Mutations in the RBD of the SARS-CoV-2 Omicron variant result in stronger binding to human ACE2 receptor [33].

In conclusion, the present 59 amino acid RBD cut fraction was found to be a good blocker of the spike-ACE2 binding. Moreover, introduced mutations especially T500S and T500G were highly potent with very high binding affinity to block the ACE2 and Omicron spike binding. The present investigation may explain that Delta variant is significantly stronger than the wild type and Omicron, while there is no significant difference between wild type and Omicron but more research is required to explore its less ability to penetrate the lung tissue. In this case, lung TMPRSS2 may have some role in viral internalization. In regard to the last 2 years' strategies, global vaccination, and natural infection, the disease outcome and severity of different new variants have become less predictable.

Supplementary Information The online version contains supplementary material available at https://doi.org/10.1007/s11224-022-02022-x.

Author contribution SM-hypothesis study design, critical analysis, and reviewing. DS-experimentation and first draft preparation.

Data availability All data are available upon reasonable requests.

Declarations

Conflict of interest The authors declare no competing interests.

References

1. WHO. WHO Coronavirus disease (COVID-19) pandemic (2021) https://www.who.int/emergencies/diseases/novel-coronavirus-2019. Accessed 7 Dec 2021
2. Shu Y, McCauley J (2017) GISAID: Global initiative on sharing all influenza data - from vision to reality. Euro Surveill 22(13):30494. https://doi.org/10.2807/1560-7917.ES.2017.22.13.30494.PMID:28382917;PMCID:PMC5388101
3. Liu C, Ginn HM, Dejnirattisai W, Supasa P, Wang B et al (2021) Reduced neutralization of SARS-CoV-2 B.1.617 by vaccine and convalescent serum. Cell. 2021 Aug 5;184(16):4220–4236.e13. https://doi.org/10.1016/j.cell.2021.06.020. Epub 2021 Jun 17. PMID: 34242578; PMCID: PMC8218332
4. GISAID Tracking of variants (2021) https://www.gisaid.org/hcov19-variants/ Date: 2021 Date accessed: November 30, 2021
5. Yang T-J, Yu P-Y, Chang Y-C et al (2021) Impacts on the structure-function relationship of SARS-CoV-2 spike by B.1.1.7 mutations. bioRxiv. Published online May 12, 2021. https://doi.org/10.1101/2021.05.11.443686
6. Chen J, Wang R, Gilby NB, Wei GW (2022) Omicron variant (B.1.1.529): infectivity, vaccine breakthrough, and antibody resistance. J Chem Inf Model. 2022 Jan 24;62(2):412–422. https://doi.org/10.1021/acs.jcim.1c01451. Epub 2022 Jan 6. PMID: 34989238; PMCID: PMC8751645
7. Graham F (2022) Daily briefing: Omicron struggles to infect the lungs. Nature. https://doi.org/10.1038/d41586-022-00039-0. Epub ahead of print. PMID: 34997237
8. Leung K, Shum MH, Leung GM, Lam TT, Wu JT (2021) Early transmissibility assessment of the N501Y mutant strains of SARS-CoV-2 in the United Kingdom, October to November 2020. Euro Surveill 26(1):2002106. https://doi.org/10.2807/1560-7917.ES.2020.26.1.2002106.Erratum.In:EuroSurveill.2021Jan;26(3):PMID:33413740;PMCID:PMC7791602
9. Korber B, Fischer WM, Gnanakaran S, Yoon H, Theiler J, Abfalterer W, Hengartner N, Giorgi EE, Bhattacharya T, Foley B, Hastie KM, Parker MD, Partridge DG, Evans CM, Freeman TM, de Silva TI; Sheffield COVID-19 Genomics Group, McDanal C, Perez LG, Tang H, Moon-Walker A, Whelan SP, LaBranche CC, Saphire EO, Montefiori DC (2020) Tracking changes in SARS-CoV-2 spike: evidence that D614G increases infectivity of the COVID-19 virus. Cell 182(4):812–827.e19. https://doi.org/10.1016/j.cell.2020.06.043. Epub 2020 Jul 3. PMID: 32697968; PMCID: PMC7332439
10. Plante JA, Liu Y, Liu J, Xia H, Johnson BA, Lokugamage KG, Zhang X, Muruato AE, Zou J, Fontes-Garfias CR, Mirchandani D, Scharton D, Bilello JP, Ku Z, An Z, Kalveram B (2021) Freiberg AN, Menachery VD, Xie X, Plante KS, Weaver SC, Shi PY. Spike mutation D614G alters SARS-CoV-2 fitness. Nature 592(7852):116–121. https://doi.org/10.1038/s41586-020-2895-3. Epub 2020 Oct 26. Erratum in: Nature. 2021 Jul;595(7865):E1. PMID: 33106671; PMCID: PMC8158177
11. Volz E, Hill V, McCrone JT, Price A, Jorgensen D, O'Toole Á, Southgate J, Johnson R, Jackson B, Nascimento FF, Rey SM, Nicholls SM, Colquhoun RM, da Silva Filipe A, Shepherd J, Pascall DJ, Shah R, Jesudason N, Li K, Jarrett R, Pacchiarini N, Bull M, Geidelberg L, Siveroni I; COG-UK Consortium, Goodfellow I, Loman NJ, Pybus OG, Robertson DL, Thomson EC, Rambaut A, Connor TR (2020) Evaluating the effects of SARS-CoV-2 spike mutation D614G on transmissibility and pathogenicity. Cell 184(1):64–75.e11. https://doi.org/10.1016/j.cell.2020.11.020. Epub 2020 Nov 19. PMID: 33275900; PMCID: PMC7674007
12. Planas D, Saunders N, Maes P, Guivel-Benhassine F, Planchais C, Buchrieser J et al (2021) Considerable escape of SARS-CoV-2 Omicron to antibody neutalization. Nature. https://doi.org/10.1038/s41586-021-04389-z. Epub ahead of print. PMID: 35016199.
13. Liu L, Iketani S, Guo Y, Chan JF, Wang M, Liu L, Luo Y, Chu H, Huang Y et al (2021) Striking antibody evasion manifested by the Omicron variant of SARS-CoV-2. Nature. https://doi.org/10.1038/s41586-021-04388-0. Epub ahead of print. PMID: 35016198
14. Nishiura H, Ito K, Anzai A, Kobayashi T, Piantham C, Rodríguez-Morales AJ (2021) Relative reproduction number of SARS-CoV-2 Omicron (B.1.1.529) compared with Delta variant in South Africa. J Clin Med 11(1):30. https://doi.org/10.3390/jcm11010030. PMID: 35011781; PMCID: PMC8745053
15. Yang G, Tan Z, Zhou L, Yang M, Peng L, Liu J, Cai J, Yang R, Han J, Huang Y, He S (2020) Effects of angiotensin II receptor blockers and ACE (angiotensin-converting enzyme) inhibitors on virus infection, inflammatory status, and clinical outcomes in patients with COVID-19 and hypertension: a single-center retrospective study. Hypertension 76(1):51–58. https://doi.org/10.1161/HYPERTENSIONAHA.120.15143 (Epub 2020 Apr 29 PMID: 32348166)

16. Science Brief (2021) Omicron (B.1.1.529) variant. CDC. Accessed December 4, 2021. https://www.cdc.gov/coronavirus/2019-ncov/science/science-briefs/scientific-brief-omicron-variant.html
17. Banerjee A, Kanwar M, Santra D, Maiti S (2021) Conserved in 186 countries the RBD fraction of SARS CoV-2 S-protein with in –silico T500S mutation strongly blocks ACE2 rejecting the viral spike: a molecular-docking analysis. bioRxiv 2021.04.25.441361. https://doi.org/10.1101/2021.04.25.441361
18. DeLano WL (2002) Pymol: an open-source molecular graphics tool CCP4 Newsletter On Protein Crystallography, 40 (2002), pp. 82–92
19. Lovell SC, Davis IW, Arendall WB 3rd, de Bakker PI, Word JM, Prisant MG, Richardson JS, Richardson DC (2003) Structure validation by Calpha geometry: phi, psi and Cbeta deviation. Proteins 50(3):437–450. https://doi.org/10.1002/prot.10286 (PMID: 12557186)
20. Honorato RV, Koukos PI, Jiménez-García B, Tsaregorodtsev A, Verlato M, Giachetti A, Rosato A, Bonvin AMJJ (2021) Structural biology in the clouds: the WeNMR-EOSC ecosystem. Front Mol Biosci 28(8):729513. https://doi.org/10.3389/fmolb.2021.729513. PMID:34395534;PMCID:PMC8356364
21. Vangone A, Bonvin AM (2015) Contacts-based prediction of binding affinity in protein-protein complexes. Elife 20(4):e07454. https://doi.org/10.7554/eLife.07454.PMID:26193119;PMCID:PMC4523921
22. López-Blanco JR, Aliaga JI, Quintana-Ortí ES, Chacón P (2014) iMODS: internal coordinates normal mode analysis server. Nucleic Acids Res 42(Web Server issue):W271–6. https://doi.org/10.1093/nar/gku339. Epub 2014 Apr 25. PMID: 24771341; PMCID: PMC4086069
23. Kabsch W (1976) A solution for the best rotation to relate two sets of vectors. Acta Crystallogr A 32:922–923
24. Damm KL, Carlson HA (2006) Gaussian-weighted RMSD superposition of proteins: a structural comparison for flexible proteins and predicted protein structures. Biophys J 90(12):4558–73. https://doi.org/10.1529/biophysj.105.066654. Epub 2006 Mar 24. PMID: 16565070; PMCID: PMC1471868
25. Maiti S, Banerjee A, Kanwar M (2021) In silico Nigellidine (N. sativa) bind to viral spike/active-sites of ACE1/2, AT1/2 to prevent COVID-19 induced vaso-tumult/vascular-damage/comorbidity. Vascul Pharmacol 138:106856. https://doi.org/10.1016/j.vph.2021.106856. Epub 2021 Mar 18. PMID: 33746069; PMCID: PMC7970800
26. Halliday D, Resnick R, Walker J (1997) Electric potential fundamentals of physics (5th ed.), John Wiley & Sons ISBN 0–471–10559–7
27. Purcell EM (2013) Electricity and magnetism Cambridge University Press (2013), pp. 16–18 ISBN 978–1107014022
28. Wu L, Zhou L, Mo M, Liu T, Wu C, Gong C, Lu K, Gong L, Zhu W, Xu Z (2022) SARS-CoV-2 Omicron RBD shows weaker binding affinity than the currently dominant Delta variant to human ACE2. Signal Transduct Target Ther 7(1):8. https://doi.org/10.1038/s41392-021-00863-2.PMID:34987150;PMCID:PMC8727475
29. Starr TN et al (2020) Deep mutational scanning of SARS-CoV-2 receptor binding domain reveals constraints on folding and ACE2 binding. Cell 182:1295-1310.e20. https://doi.org/10.1016/j.cell.2020.08.012
30. Starr TN, Greaney AJ, Hilton SK, Ellis D, Crawford KHD, Dingens AS, Navarro MJ, Bowen JE, Tortorici MA, Walls AC, King NP, Veesler D, Bloom JD (2020) deep mutational scanning of SARS-CoV-2 receptor binding domain reveals constraints on folding and ACE2 binding. Cell 182(5):1295–1310.e20. https://doi.org/10.1016/j.cell.2020.08.012. Epub 2020 Aug 11. PMID: 32841599; PMCID: PMC7418704
31. Khan K, Karim F, Cele S, San JE, Lustig G, Tegally H, Bernstein M, Ganga Y, Jule Z, Reedoy K, Ngcobo N, Mazibuko M, Mthabela N, Mhlane Z, Mbatha N, Giandhari J, Ramphal Y, Naidoo T, Manickchund N, Magula N, Karim SSA, Gray G, Hanekom W, von Gottberg A; COMMIT-KZN Team, Gosnell BI, Lessells RJ, Moore PL, de Oliveira T, Moosa MS, Sigal A (2021) Omicron infection enhances neutralizing immunity against the Delta variant. medRxiv [Preprint]. 12.27.21268439. https://doi.org/10.1101/2021.12.27.21268439. Update in: Nature PMID: 34981076; PMCID: PMC8722619
32. Syed AM, Ciling A, Khalid MM, Sreekumar B, Chen PY, Kumar GR, Silva I, Milbes B, Kojima N, Hess V, Shacreaw M, Lopez L, Brobeck M, Turner F, Spraggon L, Taha TY, Tabata T, Chen IP, Ott M, Doudna JA (2021) Omicron mutations enhance infectivity and reduce antibody neutralization of SARS-CoV-2 virus-like particles. medRxiv [Preprint]. 2022 12.20.21268048. https://doi.org/10.1101/2021.12.20.21268048. PMID: 34981067; PMCID: PMC8722610
33. Lupala CS, Ye Y, Chen H, Su XD, Liu H (2021) Mutations on RBD of SARS-CoV-2 Omicron variant result in stronger binding to human ACE2 receptor. Biochem Biophys Res Commun 590:34–41. https://doi.org/10.1016/j.bbrc.2021.12.079. Epub PMID: 34968782; PMCID: PMC8702632